JPET Fast Forward. Published on March 17, 2004 as DOI: 10.1124/jpet.104.066019

Evidence that 1,1-Dichloroethylene Induces Apoptotic Cell Death in Murine Liver

ERIK J. MARTIN and POH-GEK FORKERT

Department of Anatomy and Cell Biology, Queen's University, Kingston, Ontario, Canada

Running title: 1,1-Dichloroethylene-induced hepatic apoptosis

Address correspondence to: Dr. Poh-Gek Forkert
Department of Anatomy and Cell Biology
Queen's University
Kingston, Ontario
Canada K7L 3N6
Phone: (613) 533-2854
Fax: (613) 533-2566
E-mail: forkertp@post.queensu.ca

Text pages: 33

Tables: 0

Figures: 7

References: 40

Abstract: 250

Introduction: 618

Discussion: 1500

ABBREVIATIONS: ALT, alanine aminotransferase; CyA, cyclosporine A; DCE, 1,1-dichloroethylene; Gal/ET, galactosamine/endotoxin; JC-1, 5,5′,6,6′-tetrachloro-1,1′,3,3′-tetraethylbenzimidazolocarbocyanine iodide; MPT, mitochondrial permeability transition; PTP, permeability transition pore.

Recommended section assignment: toxicology

ABSTRACT

1,1-Dichloroethylene (DCE) causes dysfunction of hepatic mitochondria. As mitochondria have been implicated in apoptosis through opening of the permeability transition pore (PTP), we have undertaken studies to test the hypothesis that DCE induces apoptosis, in addition to necrosis, in murine liver. Our primary objective was to identify the biochemical events associated with DCE-induced apoptosis. Female CD-1 mice were treated with a mildly hepatotoxic dose of DCE (125 mg/kg, i.p.). Using the fluorescent dye JC-1, decreased hepatic mitochondrial membrane potential was detected at 2 h. Western blotting of liver cytosolic proteins showed greater immunoreactivity for cytochrome *c* in fractions from mice treated with DCE for 4 h than in controls. Furthermore, caspase-9 activity was significantly increased 6 h after DCE exposure. Immunohistochemical studies with an antibody to activated caspase-3 and TUNEL staining were used to detect apoptotic cells. In both experiments, positive reactivities were observed in centrilobular hepatocytes 12 and 24 h after DCE. Additionally, centrilobular hepatocytes showing morphological criteria of apoptosis were observed at 24 h. Apoptosis and all apoptotic events were inhibited by pretreatment for 20 min with cyclosporine A (CyA; 50 mg/kg), a specific inhibitor of the mitochondrial PTP. To determine a major role for mitochondrial permeability transition (MPT) in DCE hepatotoxicity, serum alanine aminotransferase (ALT) activity was evaluated. ALT activity was significantly elevated 2 to 24 h after DCE, and CyA failed to inhibit this activity. These data suggested that DCE produces apoptosis by inducing MPT, causing release of cytochrome *c* into the cytosol and caspase activation.

JPET Fast Forward. Published on March 17, 2004 as DOI: 10.1124/jpet.104.066019
This article has not been copyedited and formatted. The final version may differ from this version.

1,1-Dichloroethylene (DCE; vinylidene chloride) is a synthetic chemical used in the production of plastics and textiles and, as a result of its release during manufacture and use, has become a widespread environmental contaminant (U.S. EPA, 2002). Previous studies have shown that exposure to DCE causes liver injury selectively in centrilobular hepatocytes (Kanz and Reynolds, 1986; Forkert and Boyd, 2001). The lesion predominantly involved plasma membranes, nuclei and mitochondria, while the endoplasmic reticulum appeared unaffected (Kanz and Reynolds, 1986; Reynolds et al., 1984). Early morphological changes in mitochondria were manifested as swelling, disruption of cristae, and loss of mitochondrial matrix density (Kanz and Reynolds, 1986). Functional alterations in mitochondria also occur early in the toxic response to DCE. Dysfunction of these mitochondria was documented as reduced ADP-stimulated (state-3) respiration, and decreased respiratory control ratio and ADP:O ratio (Martin et al., 2003). Collectively, these findings suggested that mitochondria are a primary site of damage in DCE-mediated hepatotoxicity.

Mitochondria play a pivotal role in necrotic and apoptotic cell death through opening of the permeability transition pore (PTP) (Lemasters et al., 1998; Halestrap et al., 1998). Opening of this high-conductance inner membrane channel requires elevated cytosolic calcium levels in addition to an ‘inducing agent’, such as organic peroxides and substances that oxidize sulfhydryl groups (Crompton, 1999). Activation of the PTP causes mitochondrial swelling and uncoupling of oxidative phosphorylation that, when unrestrained, leads to necrosis (Halestrap et al., 1998; Lemasters et al., 1998). Alternatively, transient PTP opening may be involved in the induction of apoptosis by initially causing mitochondrial swelling followed by rupture or permeabilization of the

outer membrane thus releasing cytochrome *c* into the cytosol (Halestrap et al., 1998, 2000). Once released, cytochrome *c* triggers the assembly of the apoptosome, a multimeric structure composed of cytochrome *c*, apoptotic protease activating factor 1 (APAF-1), and ATP or dATP. This complex recruits and activates procaspase-9, a prolific initiator caspase that subsequently cleaves and activates procaspase-3 (Hengartner, 2000). Caspase-3, a potent downstream effector caspase, induces the proteolytic cleavage of a range of target proteins responsible for the rearrangement of the cytosol, nucleus and plasma membrane characteristic of apoptosis (Kluck et al., 1997; Li and Yuan, 1999; Zimmermann et al., 2001).

A number of compounds are postulated to cause hepatocellular death by both necrosis and apoptosis, including acetaminophen (Ray et al., 1996) and galactosamine (Gujral et al., 2003). Although the precise mechanism(s) of DCE-induced liver injury has not clearly been delineated, centrilobular necrosis is well documented while studies characterizing apoptosis are rudimentary. Previous investigations have demonstrated covalent binding of DCE metabolites in fractions of mitochondria, endoplasmic reticulum (ER), and plasma membranes (Okine et al., 1985), organelles responsible for maintenance of calcium and cellular energy homeostasis. Additionally, it has been shown that DCE inhibits calcium sequestration by the Ca^{2+}/Mg^{2+} ATPase in rat liver ER (Moore, 1982). Moreover, cytosolic calcium accumulation was observed in hepatocyte suspensions after DCE exposure (Long and Moore, 1987). Increased cytosolic calcium concentrations and mitochondrial dysfunction are both conditions intrinsic to apoptotic cell death. Furthermore, following DCE administration, scattered individual hepatocytes were observed in rat livers showing nuclear and cytoplasmic alterations typical of

apoptosis (Reynolds et al., 1984). In this investigation, we have undertaken studies to test the hypothesis that apoptosis is an important and currently unexplained process in DCE-mediated hepatotoxicity. Our primary objective was to examine the biochemical events associated with this mode of cell death, including MPT induction, cytochrome *c* release and activation of caspases-9 and -3. Additionally, we have investigated the occurrence of DCE-induced apoptosis and its relationship to necrosis, using the TUNEL assay and histopathological evaluation. Furthermore, we have examined the role of mitochondrial permeability transition (MPT) in elaboration of DCE-mediated apoptosis using cyclosporine A, a specific inhibitor of PTP.

JPET Fast Forward. Published on March 17, 2004 as DOI: 10.1124/jpet.104.066019
This article has not been copyedited and formatted. The final version may differ from this version.

Materials and Methods

Chemicals and Reagents. Chemicals and reagents were purchased from suppliers as follows: 1,1-dichloroethylene (vinylidene chloride; >99% purity) (Aldrich Chemical Co., Montreal, Quebec, Canada); anti-cytochrome *c* (BD Biosciences Canada, Mississauga, ON); Bio-Rad protein assay dye reagent concentrate (Bio-Rad Laboratories, Hercules, CA); cyclosporine A (Calbiochem, San Diego, CA); peroxidase-conjugated goat anti-mouse IgG (Jackson Immunoresearch Laboratories Inc., West Grove, PA); 5,5′,6,6′-tetrachloro-1,1′,3,3′-tetraethylbenzimidazolocarbocyanine iodide (JC-1) (Molecular Probes Inc., Eugene, OR); bovine serum albumin (BSA), collagenase type I, D(+)-galactosamine, horse serum, Leibovitz L-15 medium, lipopolysaccharide (endotoxin), Hanks' balanced salt solution (modified), trypan blue solution (0.4%) (Sigma Chemical Co., St. Louis, MO); avidin/biotin blocking kit, streptavidin-peroxidase (Zymed Laboratories Inc., San Francisco, CA). All other chemicals were of reagent grade and were obtained from standard commercial suppliers.

Animal Treatment. Female CD-1 mice (25-30 g) were obtained from Charles River Canada (St. Constant, Quebec, Canada). They were maintained on a 12 h light/dark cycle and given free access to food (Purina Rodent Chow; Ralston Purina International, Strathroy, Ontario, Canada) and drinking water. Following acclimatization to laboratory conditions for at least 5 d, mice were randomly assigned to control or treatment groups (n = 3). In all experiments, mice were treated intraperitoneally (i.p.) with 125 mg/kg DCE in corn oil. This dose has previously been shown to produce mitochondrial dysfunction and mild centrilobular necrosis in murine liver (Martin et al., 2003; Forkert and Boyd, 2001). For studies that examined the effects of CyA (50 mg/kg in corn oil, i.p.), CyA

was administered 20 min prior to treatment with DCE for 24 h (CyA + DCE). In other investigations, this dose of CyA has been shown to inhibit apoptotic cell death (Sugie et al., 2002). In flow cytometry studies, mice were treated with DCE, DCE and CyA, or 700 mg/kg galactosamine and 100 μg/kg endotoxin (Gal/ET, i.p.) for 2 h, as mitochondrial dysfunction has been shown to peak at this time (Martin et al., 2002). Mice were then anesthetized for perfusion and hepatocyte isolation. Gal/ET has been shown to produce extensive hepatocellular apoptosis in mice (Jaeschke et al., 1998; Gujral et al., 2002) and was used as a positive control. For detection of cytochrome *c* in cytosol and measurement of caspase-9 protease activity, mice were treated for 4 h and 6 h, respectively, with DCE or DCE and CyA. These mice were sacrificed by cervical dislocation. For measurements of serum alanine aminotransferase (ALT) activity, mice were treated with DCE or DCE and CyA for 0.5, 1, 2, 4, 8, 12, 18, and 24 h. Mice were then anesthetized with sodium pentobarbital (120 mg/kg; i.p.), and intracardiac blood was obtained for assessment of ALT activity. For immunohistochemical, hematoxylin and eosin (H & E), and TUNEL staining experiments, mice were treated with DCE for 12 or 24 h, CyA + DCE, or Gal/ET for 6 h, and then anesthetized for perfusion. In all studies, control mice were treated with equivalent volumes of the appropriate vehicle and were sacrificed at times corresponding to those in the experimental groups.

Preparation of Isolated Hepatocytes. Hepatic parenchymal cells were isolated by the method of Klaunig et al. (1981), with modifications. Briefly, mice were perfused with calcium- and magnesium-free Hanks' balanced salt solution containing 0.5 mM EGTA and 50 mM HEPES (pH 7.3) and then with Leibovitz modified L15 medium (pH 7.4) containing collagenase (100 U/ml), both maintained at 37˚C. Livers were then excised

and transferred to a petri dish containing 15 ml of collagenase perfusate. Hepatocytes were gently stripped from the connective tissue stroma using a spatula and further separated by repeated pipetting through a single thickness of nylon mesh fabric (Millipore, Bedford, MA). Cells were subsequently pelleted at 50 *g* for 1 min at 10˚C and then resuspended in 20 ml of modified L15 medium containing BSA (0.2% w/v) and horse serum (10% v/v). Initial cell viability was measured in a hemocytometer by trypan blue dye (0.4%) exclusion and was found to be greater than 90%.

Measurement of Hepatocyte Mitochondrial Membrane Potential. Mitochondrial membrane potential in intact liver cells was assessed using the mitochondrial specific fluorescent probe JC-1, based on the method of Reers et al. (1995). JC-1 exists as a green-fluorescing monomer at low membrane potentials (<120 mV) and as a red-fluorescing dimer (J-aggregate) at membrane potentials greater than 180 mV. Following excitation at 488 nm, the ratio of red (595-nm emission) to green (525-nm emission) fluorescence measures the ratio of high-to-low mitochondrial membrane potential (Reers et al., 1995). Hepatocytes (10^6 cells/ml L15 medium containing BSA and horse serum) were incubated with JC-1 (5.0 µM) for 25 min at 37˚C in the dark, with gentle agitation. Cells were then washed twice with fresh media and resuspended in a total volume of 10 ml. To measure the basal fluorescence of each cell preparation, an aliquot was removed prior to the addition of JC-1 and measured cytofluorometrically. Thus, each mouse liver yielded one aliquot (10 ml; 10^6 cells/ml) for sample reading and one aliquot (5 ml; 10^6 cells/ml) for reading of basal fluorescence.

Analysis of cell samples was performed using a Coulter Epics Altra flow cytometer equipped with a Coherent Enterprise water-cooled, 488-nm argon laser. The settings for

the detection system were as follows: channel 1 dichroic, 488-nm mirror longpass; channel 1 bandpass, 488-nm bandpass; channel 2 block, 488-nm block; channel 2 dichroic, 550-nm dichroic mirror longpass; channel 2 bandpass, 525-nm bandpass; channel 3 dichroic, 600-nm dichroic mirror longpass; and channel 3 bandpass, 595-nm bandpass. Mean red and green fluorescence intensities of a minimum of 10,000 cells/sample were analyzed with EXPO32 flow cytometry software.

Protein Immunoblotting. Mitochondrial cytochrome *c* release was evaluated by Western blotting as previously described (Lee et al., 1998), with minor modifications. Briefly, livers of mice were excised, rinsed, blotted, and weighed. Cytosolic fractions were then prepared (Forkert, 1999), aliquoted, frozen in liquid nitrogen, and stored at -70˚C. Protein concentrations were determined using the Bradford protein assay (Bradford, 1976). Cytosolic proteins (25 µg per lane) were separated electrophoretically on a 15% SDS-polyacrylamide gel and then transferred to a polyvinylidene difluoride (PVDF) membrane filter. The membrane was then rinsed with tris-buffered saline (TBS) and blocked for 2 h with 5% nonfat dried milk diluted in TBS. After thorough washing in Tween 20-TBS (T/TBS), the membrane was reacted overnight at 4˚C with a monoclonal antibody directed against cytochrome *c* (1:500). The membrane was again washed with T/TBS to remove unbound antibodies and then reacted with a secondary antibody (goat anti-mouse IgG conjugated to horseradish peroxidase, 1:7,500) for 2 h at room temperature (RT). The antibodies were diluted in T/TBS containing 1% nonfat dried milk. Proteins were visualized using an Immun-Star HRP chemiluminescence kit (Bio-Rad Laboratories Inc., Hercules, CA). Densitometric analysis of the gels was performed using SigmaGel software (Sigma-Aldrich Corp., St. Louis, MO).

Measurement of ALT Activity. Serum ALT activity was measured by the method of Bergmeyer et al. (1978) using an ALT 20 kit (Sigma Diagnostics Inc., St. Louis, MO). ALT activity was determined at 0.5, 1, 2, 4, 8, 12, 18, and 24 h after DCE (125 mg/kg) or DCE and CyA (50 mg/kg) treatment.

Measurement of Caspase-9 Protease Activity. Hepatic caspase-9 activity was measured using an ApoAlert Caspase Fluorescent Assay Kit (Clontech Laboratories Inc., Palo Alto, CA), with minor modifications. Briefly, approximately 100 mg of freshly isolated liver was homogenized in a hypoosmotic lysing buffer (10 mM Tris-HCL, 10 mM $NaH_2PO_4/NaHPO_4$, 130 mM NaCl, 1% Triton X-100, 10 mM PPi, pH 7.5). After being placed on ice for 30 min, the homogenate was centrifuged (14,500 *g*) for 30 min at 4˚C. The supernatant was used for the enzyme assay. This extraction procedure releases all of the soluble proteins into the supernatant regardless of their intracellular localization. Enzyme activity was assayed on 0.2-0.7 mg of protein per sample in a reaction medium containing a caspase-9 substrate; Leu-Glu-His-Asp-7-amino-4-methyl coumarin (LEHD-AMC). In some assays, a caspase-9 inhibitor (LEHD-CHO; 0.05 mM final concentration) was included in addition to the substrate to ensure specificity of the protease activity. Fluorometric detection was performed with a SpectraMax microplate reader using a 380-nm excitation filter and 460-nm emission filter (Molecular Devices Corp., Sunnyvale, CA).

Immunohistochemical Detection of Caspase-3. Liver tissue was prepared for immunohistochemical evaluation as previously described (Forkert, 1999), with minor modifications. Briefly, livers were fixed by vascular perfusion through the left ventricle with 4% paraformaldehyde in 0.1 M Sorenson's buffer (12.0 mM NaH_2PO_4, 69.0 mM

Na_2HPO_4, pH 7.4). Tissues were processed and embedded in paraffin using standard procedures. Tissue sections (5 µm) were deparaffinized, cleared, and hydrated. After rinsing in PBS, the sections were blocked in 5% normal goat serum (NGS) for 20 min. After further rinsing in PBS, the sections were incubated for 10 min at RT with avidin and then biotin to block any endogenous biotin. Tissue sections were subsequently incubated overnight in rabbit anti-active caspase-3 polyclonal antiserum (Cell Signaling Technology Inc., Beverly, MA). The antiserum was diluted 1:200 in PBS containing 2.5% NGS. The sections were rinsed thoroughly to remove unbound antibodies, and were reacted with biotinylated goat anti-rabbit IgG for 10 min at RT. Endogenous peroxidase activity was blocked by incubating tissue sections for 30 min with 1% hydrogen peroxide in nanopure water. Sections were then reacted with streptavidin conjugated to horseradish peroxidase for 10 min, and the immunoperoxidase color reaction was developed using a DAKO liquid DAB kit (DAKO Corp., Carpinteria, CA). The tissue sections were then counterstained in hematoxylin, dehydrated, cleared, and mounted. Incubations were also performed in the absence of the specific antibody to control for the specificity of the immunohistochemical reaction.

TUNEL Assay. DNA fragmentation characteristic of apoptosis was examined using a TdT (terminal deoxynucleotidyl transferase)-FragEL Kit (Oncogene Research Products, San Diego, CA). Briefly, 4% paraformaldehyde-fixed tissue samples were embedded in paraffin and 5-µm sections were obtained. Replicate sections were rehydrated and permeabilized with proteinase K (20 µg/ml) for 20 min at RT. Next, endogenous peroxidases were inactivated by covering the sections with 3% H_2O_2 for 5 min. After incubation for 5 min in TdT buffer (200 mM Na-cacodylate, 30 mM Tris, 0.3 mg/ml

BSA, 0.75 mM $CoCl_2$, pH 6.6), the slides were covered with TdT and biotinylated dUTP and incubated for 1.5 h at 37˚C in a humidified chamber. Negative controls were incubated with biotinylated dUTP in TdT buffer in the absence of enzyme. The reaction was terminated by covering the sections with stop buffer (0.5 M EDTA, pH 8.0) for 5 min at RT. After blocking in BSA (4%), the slides were incubated with a streptavidin-horseradish peroxidase conjugate for 30 min. The sections were then incubated in diaminobenzidine (DAB) for 12 min at RT and counterstained with methyl green. Apoptotic cells were identified by staining properties and by morphological criteria (cell shrinkage, chromatin condensation and/or margination, apoptotic bodies).

Histopathology. Liver tissue was prepared for histopathological evaluation as previously described (Forkert and Boyd, 2001). Briefly, livers were fixed by vascular perfusion through the left ventricle with 4% paraformaldehyde in 0.1 M Sorenson's phosphate buffer, pH 7.4. Tissues were processed and embedded in paraffin using standard procedures. Liver sections (5 µm) were stained with hematoxylin and eosin.

Statistical Analysis. Data are expressed as mean ± standard deviation (S.D.). Statistical analysis was performed by one-way analysis of variance (ANOVA) followed by Tukey's test to determine significant differences between experimental groups ($p < 0.05$).

Results

Measurement of Mitochondrial Membrane Potential. Hepatocyte mitochondrial transmembrane potential ($\Delta\Psi_m$) was assessed 2 h after treatment with DCE or DCE and CyA using the fluorescent probe JC-1. As indicated by JC-1 fluorescence ratios, DCE caused substantial disruption of mitochondrial membrane potential (Fig. 1). The alterations in fluorescence were similar to those caused by Gal/ET treatment for 4 h. Pretreatment with CyA significantly inhibited DCE-induced disruption of mitochondrial membrane potential.

Immunochemical Detection of Cytochrome *c*. Protein immunoblotting of liver cytosol for cytochrome *c* revealed a single band of approximately 15 kDa in all samples (Fig. 2). This is similar to the apparent molecular mass of cytochrome *c* identified in other studies (Knight and Jaeschke, 2002). At 4 h, immunoreactive protein was augmented in cytosolic fractions from DCE-treated mice compared to fractions from untreated animals; however, these increases were abrogated by pretreatment with CyA. Densitometric analysis of the protein bands showed that the amounts of cytochrome *c* in cytosolic fractions from DCE-treated mice were approximately 3-fold higher than in those from untreated mice. Pretreatment with CyA diminished the DCE-induced increases of cytochrome *c* to approximately 2-fold of control levels.

Measurement of ALT Activity. DCE-induced hepatotoxicity and the protective effects of CyA were temporally assessed by measurement of serum ALT activity. ALT activity was found to be significantly elevated from 2 to 24 h after DCE, as compared to controls (Fig. 3). Pretreatment with CyA failed to inhibit DCE-induced increases in serum ALT activity at any time point.

Measurement of Caspase-9 Protease Activity. Caspase-9 protease activity was assessed by cleavage of the peptide substrate LEHD-AMC in modified liver homogenates. Conjugated AMC emits in the UV range (λ_{max}=380 nm); however, after proteolytic cleavage by caspase-9, free AMC fluoresces green (460 nm). Protease activity was found to be significantly increased at 6 h after DCE (125 mg/kg) (Fig. 4). Pretreatment with CyA inhibited the elevations in caspase-9 activity observed after DCE treatment. To verify that the signal detected was due to caspase-9 protease activity, samples from DCE treated animals were incubated with caspase-9 inhibitor. Here, caspase-9 activity was similar to that in control samples.

Immunohistochemical Localization of Activated Caspase-3. Immunohistochemical studies were performed on liver tissues to detect activated caspase-3; one of the key executioners of apoptosis (Hengartner, 2000). Staining of cleaved caspase-3 is characteristically localized in the cytoplasm and perinuclear region of apoptotic cells. In liver sections from control mice, specific staining was not apparent (Fig. 5A). However, in sections from mice treated with DCE (125 mg/kg) for 12 or 24 h, staining was observed in centrilobular hepatocytes, although a few individual cells in other areas of the hepatic lobule were also stained (Fig. 5, C and D). Moreover, staining for activated caspase-3 appeared to increase from 12 to 24 h. In liver sections from mice treated with CyA + DCE, sparse hepatocyte staining was observed in centrilobular regions (Fig. 5E). In sections from mice treated with Gal/ET for 6 h, numerous positively-stained hepatocytes were seen scattered throughout the parenchyma (Fig. 5B). In all tissue sections, the majority of stained cells showed some morphological characteristics of apoptosis (i.e. cell shrinkage, chromatin condensation and/or margination, and apoptotic

bodies). In sections from DCE-, CyA + DCE-, and Gal/ET-treated mice where the specific antibody was omitted, hepatocyte staining was rare.

TUNEL Assay. The TUNEL assay was used to detect hepatic DNA fragmentation characteristic of apoptosis. In control liver sections, TUNEL-positive cells were rare (Fig. 6A). However, in sections from mice treated with DCE (125 mg/kg) for 12 or 24 h, confluent TUNEL staining was observed in centrilobular regions, although a few individual cells in other areas of the parenchyma were also stained (Fig. 6, C and D). Moreover, TUNEL staining appeared to increase from 12 to 24 h. In liver sections from mice treated with CyA + DCE, TUNEL staining was observed in centrilobular regions (Fig. 6 E). Here, staining was similar to that observed after DCE for 24 h, but confined to centrilobular hepatocytes. Sections of liver tissue from mice treated with Gal/ET for 6 h showed numerous positively-stained hepatocytes (Fig. 6B). These stained cells were distributed throughout the tissue and all showed morphological characteristics of apoptosis. The staining pattern of hepatocytes in Gal/ET sections was different from that observed in sections from DCE- or CyA + DCE-treated animals. Positively stained cells after Gal/ET treatment had distinct nuclear staining, whereas hepatocytes after DCE or CyA + DCE showed diffuse staining in the cytosol and nucleus. In sections from DCE-, CyA + DCE-, and Gal/ET-treated mice where TdT enzyme was omitted, TUNEL staining was rare.

Histopathology. Histopathological evaluation was performed in liver tissue 12 and 24 h after treatment with DCE (125 mg/kg). Hepatocellular injury was not observed in mice treated with DCE for 12 h, compared with liver structure of the controls (Fig. 7, A and B). However, treatment with DCE for 24 h elicited mild centrilobular necrosis and

eosinophilia (Fig. 7, C and D). Additionally, some centrilobular hepatocytes showed typical morphological characteristics of apoptosis, including cell shrinkage, retraction of cell borders, and chromatin condensation and margination (Fig. 7D). In liver sections from mice treated with CyA + DCE, apoptotic and necrotic hepatocytes were observed in centrilobular regions; however, CyA pretreatment greatly reduced the number of hepatocytes undergoing apoptosis (Fig. 7E). In sections from mice treated with Gal/ET for 6 h, many apoptotic hepatocytes were observed scattered throughout the parenchyma (Fig. 7F).

Discussion

The hepatotoxic lesion induced by DCE is manifested in centrilobular hepatocytes and involves several cellular organelles, including plasma membranes, nuclei and mitochondria (Reynolds et al., 1980; Kanz and Reynolds, 1986; Forkert and Boyd, 2001). Here, we document the occurrence of hepatocellular apoptosis and its relationship to necrosis following acute exposure to DCE. Several approaches were applied to elucidate the molecular mechanisms involved in this mode of cell death. Our results suggested that DCE produces apoptotic cell death by inducing MPT, causing release of cytochrome *c* into the cytosol and caspase activation.

Apoptosis is mediated through two major pathways, the extrinsic 'death receptor' pathway (Hengartner, 2000) and the intrinsic mitochondrial pathway (Kroemer and Reed, 2000). The extrinsic pathway is initiated by ligand binding and subsequent clustering of plasma membrane death-receptors. This event leads to sequential recruitment of adaptors and initiator caspases (i.e. caspase-8 and -10) into the death-inducing signaling complex that ultimately mediates cell death (Hengartner, 2000). Alternatively, the intrinsic mitochondrial pathway is triggered by various extracellular and/or internal stress cues, such as perturbations of calcium homeostasis, DNA damage and oxidative stress. These signals can directly or indirectly induce MPT, setting the apoptotic cascade in motion (Kroemer and Reed, 2000). Previous investigations have demonstrated early increases of cytosolic calcium levels following DCE exposure (Long and Moore, 1987). In other studies, structural and functional perturbations of mitochondria have been reported (Kanz and Reynolds, 1986; Martin et al., 2003). Furthermore, morphological alterations characteristic of apoptosis were observed in scattered hepatocytes of rats after DCE

administration (Reynolds et al., 1984). Taken together, these data suggested that DCE induces the intrinsic mitochondrial pathway, and several features of this apoptotic pathway were investigated in this study.

MPT reflects a sudden increase in permeability of the inner mitochondrial membrane, resulting in membrane depolarization, uncoupling of oxidative phosphorylation, mitochondrial swelling, and release of various soluble intermembranous proteins includinhg cytochrome *c* (Lemasters, 1998). MPT is regulated by a voltage-dependent channel that is inhibited by nanomolar concentrations of cyclosporine A (Seaton et al., 1998). To assess DCE-mediated induction of MPT, the mitochondrial membrane potential ($\Delta\Psi_m$) and release of cytochrome *c* to the cytosol were determined. The $\Delta\Psi_m$, measured, using the cationic dye JC-1, was found to be significantly decreased 2 h after DCE (Fig. 1). Interestingly, this is the same time-point at which uncoupling of oxidative phosphorylation was maximal (Martin et al., 2003). Additionally, cytosolic levels of cytochrome *c* were 3-fold greater in livers from mice treated with DCE for 4 h than in controls (Fig. 2). Moreover, CyA pretreatment significantly inhibited DCE-induced disruptions of $\Delta\Psi_m$ and release of cytochrome *c* (Figs. 1 and 2). These findings are consistent with the premise that DCE activates the intrinsic mitochondrial pathway of apoptosis in which MPT precedes release of cytochrome *c* to the cytosol.

To support a major role for MPT in the mechanism of DCE hepatotoxicity, serum ALT activity was temporally assessed following DCE or DCE and CyA treatment. DCE treatment significantly increased ALT activity from 2 to 24 h, indicative of hepatocellular damage (Fig. 3). Pretreatment with CyA failed to inhibit these increases in serum ALT activity at any time point. Thus, these data do not support a major role for MPT in

overall DCE hepatotoxicity. In recent studies, elevated levels of serum ALT activity have been reported following in vivo induction of hepatic apoptosis (Segawa, 2001). These studies are intriguing as increases in serum ALT activity have classically been associated with necrotic cell death. However, in the current investigation, CyA had no effect on DCE-induced increases in serum ALT activity suggesting that elevations in activity are the result of necrotic cell death and not apoptosis.

Extensive investigation into the signaling mechanisms of the mitochondrial pathway of apoptosis demonstrated a critical role for the caspase family of cysteine proteases (Hengartner, 2000). The proteolytic activity of these enzymes accounts for many of the characteristic morphological features of apoptosis, including nuclear shrinking, chromatin condensation, and cytoplasmic blebbing (Rao et al., 1996; Rudel and Bokoch, 1997; Liu et al., 1997). Previous studies have shown that mitochondrial release of cytochrome *c* triggers the assembly of the apoptosome, a multimeric structure that recruits and activates procaspase-9, a prolific initiator caspase (Hengartner, 2000). The primary function of caspase-9 is processing of procaspase-3 to generate caspase-3. Once activated, this executioner caspase initiates a chain of reactions from which there is no return to the non-apoptotic state of the cell (Cohen, 1997). In the present study, levels of caspase-9 activity were significantly elevated 6 h following DCE administration (Fig. 4). Furthermore, activated caspase-3 was detected primarily in centrilobular hepatocytes, while a few individual cells were stained in other regions of the hepatic parenchyma (Fig. 5). As CyA pretreatment inhibited caspase-9 activity and decreased staining for caspase-3, these data again implicated MPT in the sequence of events leading to DCE-induced apoptosis. Because apoptosis is an ongoing physiological process, tissues often display basal levels

of activated enzyme. This contention is supported by the results of this study wherein basal levels of caspase-9 activity and caspase-3 staining were observed. Collectively, these data supported a role for caspase-9 and caspase-3 in the elaboration of DCE-induced apoptosis.

Additional insight into the pathogenesis of DCE-mediated hepatotoxicity was gained from TUNEL staining and histopathological assessment. TUNEL staining can be used to detect both apoptosis and necrosis as both modes of cell death involve internucleosomal DNA cleavage (Tateyama et al., 1998). However, apoptotic cells exhibit distinct nuclear staining whereas necrotic cells display diffuse staining in the cytosol and nucleus (Gujral et al., 2003). TUNEL staining in the cytosol of necrotic cells may result from nuclear degradation and leakage of cleaved DNA to the cytosol. In mice treatment with DCE for 12 or 24 h, TUNEL staining was observed predominantly in centrilobular hepatocytes while a few cells were stained in other areas of the tissue (Fig. 6). All of the TUNEL-positive cells showed diffuse cytoplasmic staining while nuclear staining varied from moderate to intense, suggesting a necrotic mode of cell death. However, when H & E stained liver sections were evaluated 24 h after DCE, apoptotic and necrotic hepatocytes were observed concomitantly in the centrilobular region (Fig. 7). Apoptotic cells exhibited characteristic morphological features of apoptosis, including cell shrinkage and chromatin condensation and margination. CyA pretreatment greatly reduced the number of histologically observable hepatocytes undergoing apoptosis supporting the notion that MPT induction is an important event in DCE-induced apoptosis. These data are consistent with previous ultrastructural studies in rats in which morphological features of both apoptotic and necrotic cell death were observed after DCE administration (Reynolds

et al., 1984). Thus, it is possible that TUNEL-positive centrilobular hepatocytes demonstrating intense nuclear staining represent a population of damaged cells undergoing apoptosis.

Recent debate has questioned whether apoptosis and necrosis are indeed two separate modes of cell death. As evidence for a unified cell death pathway, studies have shown that MPT may be a critical event in both apoptosis and necrosis (Lemasters et al., 1999). Since apoptosis is an energy-requiring process, ATP depletion may interrupt the apoptotic signaling cascade, leading to secondary necrosis (Leist, 1997). Thus, it was postulated that cellular ATP content following MPT induction determines whether a cell dies by apoptosis or necrosis (Lemasters et al., 1999). However, data from the current study suggested that DCE induces apoptosis independent of necrosis. This conclusion is supported by the observation that CyA, despite its effectiveness in preventing apoptosis, had no significant effect on necrosis.

Although the present investigation indicates that DCE induces both apoptosis and necrosis, the initiating events leading to either mode of cell death are unclear. It is conceivable that DCE-derived metabolites arylate and/or oxidize organellar proteins essential for the maintenance of calcium homeostasis. Indeed, studies have demonstrated covalent binding of DCE metabolites in fractions of mitochondria, endoplasmic reticulum (ER), and plasma membranes (Okine et al., 1985). Furthermore, it has been shown that DCE inhibits calcium sequestration by the Ca^{2+}/Mg^{2+} ATPase in rat liver ER (Moore, 1982). Moreover, cytosolic calcium accumulation was observed in hepatocyte suspensions after DCE exposure (Long and Moore, 1987). Because high cytosolic calcium concentrations are closely associated with induction of MPT, DCE may initiate

apoptosis through this mechanism. Alternately, an increase in cytosolic calcium levels may activate a number of calcium-dependent hepatic enzymes, including lipases, proteases and endonucleases, that could cause irreversible damage to cell constituents and ultimately lead to cell necrosis. Studies to date have excluded endonuclease activation as an early event in DCE hepatotoxicity (Long et al., 1989); however, further investigation is necessary to determine if other degradative enzymes contribute to toxicity. Thus, a calcium-mediated mechanism of cell injury could explicate both apoptotic and necrotic cell death following DCE exposure.

In conclusion, this investigation provides for the first time mechanistic data supporting hepatocellular apoptosis as a mode of cell death in DCE hepatotoxicity. Here, MPT induction, cytochrome *c* release and caspase activation appear to be important events in the apoptotic cascade. Additionally, apoptotic cell death was shown to occur concurrently with necrosis, the mode of cell death classically associated with DCE hepatotoxicity.

Acknowledgments

We thank Jeffrey Mewburn for his assistance in the flow cytometry studies. The technical assistance provided by Kathy Collins and Brandie Millen is gratefully acknowledged.

References

Bergmeyer HU, Scheibe P and Wahlefeld AW (1978) Optimization of methods for aspartate aminotransferase and alanine aminotransferase. *Clin Chem* **24:**58.

Bradford MM (1976) A rapid and sensitive method for the quantitation of microgram quantities of protein using the principle of protein-dye binding. *Anal Biochem* **72:**248-254.

Cohen GM (1997) Caspases: the executioners of apoptosis. *Biochem J* **326:**1-16.

Crompton M (1999) The mitochondrial permeability transition pore and its role in cell death. *Biochem J* **341:**233-249.

Forkert PG and Boyd SM (2001) Differential metabolism of 1,1-dichloroethylene in livers of A/J, CD-1, and C57BL/6 mice. *Drug Metab Dispos* **29:**1396-1402.

Forkert PG (1999) In vivo formation and localization of 1,1-dichloroethylene epoxide in murine liver: identification of its glutathione conjugate 2-*s*-glutathionyl acetate. *J Pharmacol Exp Ther* **290:**1299-1306.

Gujral JS, Farhood A and Jaeschke H (2003) Oncotic necrosis and caspase-dependent apoptosis during galactosamine-induced liver injury in rats. *Toxicol Appl Pharmacol* **190:**37-46.

Gujral JS, Knight TR, Farhood A, Bajt ML and Jaeschke H (2002) Mode of cell death after acetaminophen overdose in mice: apoptosis or oncotic necrosis? *Toxicol Sci* **67:**322-328.

Halestrap AP, Doran E, Gillespie JP and O'Toole A (2000) Mitochondria and cell death. *Biochem Soc Trans* **28:**170-177.

Halestrap AP, Kerr PM, Javadov S and Woodfield KY (1998) Elucidating the molecular mechanism of the permeability transition pore and its role in reperfusion injury of the heart. *Biochim Biophys Acta* **1366:**79-94.

Hengartner MO (2000) The biochemistry of apoptosis. *Nature* **407:**770-776.

Jaeschke H, Fisher MA, Lawson JA, Simmons CA, Farhood A and Jones DA (1998) Activation of caspase-3 (CPP32)-like proteases is essential for TNF-α-induced hepatic parenchymal cell apoptosis and neutrophil-mediated necrosis in a murine endotoxin shock model. *J Immunol* **160:**3480-3486.

Kanz MF and Reynolds ES (1986) Early effects of 1,1-dichloroethylene on canalicular and plasma membranes: ultrastructure and stereology. *Exp Mol Pathol* **44:**93-110.

Klaunig JE, Goldblatt PJ, Hinton DE, Lipsky MM, Chacko J and Trump BF (1981) Mouse liver cell culture. I. Hepatocyte isolation. *In Vitro* **17:**913-925.

Kluck RM, Bossy-Wetzel E, Green DR and Newmeyer DD (1997) The release of cytochrome c from mitochondria: a primary site for bcl-2 regulation of apoptosis. *Science* **275:**1132-1136.

Knight TR and Jaeschke H (2002) Acetaminophen-induced inhibition of fas receptor-mediated liver cell apoptosis: mitochondrial dysfunction versus glutathione depletion. *Toxicol Appl Pharmacol* **181:**133-141.

Kroemer G and Reed JC (2000) Mitochondrial control of cell death. *Nature Med* **6:**513-519.

Lee RP, Parkinson A and Forkert PG (1998) Isozyme-selective metabolism of ethyl carbamate by cytochrome P450 (CYP2E1) and carboxylesterase (hydrolase A) enzymes in murine liver microsomes. *Drug Metab Dispos* **26:**60-65.

Leist M, Single B, Castoldi AF, Kuhnle S and Nicotera P (1997) Intracellular adenosine triphosphate (ATP) concentration: A switch in the decision between apoptosis and necrosis. *J Exp Med* **185:**1481-1486.

Lemasters JJ (1999) Necrapoptosis and the mitochondrial permeability transition: shared pathways to necrosis and apoptosis. *Am J Physiol* **276:**G1-G6.

Lemasters JJ, Nieminen AL, Qian T, Trost LC, Elmore SP, Nishimura Y, Crowe RA, Cascio WE, Bradham CA, Brenner DA and Herman B (1998) The mitochondrial permeability transition in cell death: a common mechanism in necrosis, apoptosis and autophagy. *Biochim Biophys Acta* **1366:**177-196.

Li HL and Yuan JY (1999) Deciphering the pathways of life and death. *Curr Opin Cell Biol* **11:**261-266.

Liu X, Zou H, Slaughter C and Wang X (1997) DFF, a heterodimeric protein that functions downstream of caspase-3 to trigger DNA fragmentation during apoptosis. *Cell* **89:**175-184.

Long RM and Moore L (1987) Cytosolic calcium after carbon tetrachloride, 1,1-dichloroethylene, and phenylephrine exposure. *Biochem Pharmacol* **36:**1215-1221.

Long RM, Moore L and Schoenberg (1989) Halocarbon hepatotoxicity is not initiated by Ca^{2+}-stimulated endonuclease activation. *Toxicol Appl Pharmacol* **97:**350-359.

Martin EJ, Racz WJ and Forkert PG (2003) Mitochondrial dysfunction is an early manifestation of 1,1-dichloroethylene-induced hepatotoxicity in mice. *J Pharmacol Exp Ther* **304:**121-129.

Moore L (1982) 1,1-Dichloroethylene inhibition of liver endoplasmic reticulum calcium pump function. *Biochem Pharmacol* **31:**1463-1465.

Okine LK, Goochee JM and Gram TE (1985) Studies on the distribution and covalent binding of 1,1-dichloroethylene in the mouse. *Biochem Pharmacol* **34:**4051-4057.

Rao L, Perez D and White E (1996) Lamin proteolysis facilitates nuclear events during apoptosis. *J Cell Biol* **135:**1441-1455.

Ray S, Mumaw VR, Raje RR and Fariss MW (1996) Protection of acetaminophen-induced hepatocellular apoptosis and necrosis by cholesteryl hemisuccinate pretreatment. *J Pharmacol Exp Ther* **279:**1470-1483.

Reers M, Smiley ST, Mottola-Hartshorn C, Chen A, Lin M and Chen LB (1995) Mitochondrial membrane potential monitored by JC-1 dye. *Methods Enzymol* **260:**406-417.

Reynolds ES, Kanz MF, Chieco P and Moslen MT (1984) 1,1-Dichloroethylene: an apoptotic hepatotoxin? *Environ Health Perspect* **57:**313-320.

Reynolds ES, Moslen MT, Boor PJ and Jaeger RJ (1980) 1,1-Dichloroethylene hepatotoxicity. Time course of GSH changes and biochemical aberrations. *Am J Pathol* **101:**331-344.

Rudel T and Bokoch GM (1997) Membrane and morphological changes in apoptotic cells regulated by caspase-mediated activation of PAK2. *Science* **276:**1571-1574.

Seaton TA, Cooper JM and Schipra AHV (1998) Cyclosporin inhibition of apoptosis by mitochondrial complex I toxins. *Brain Res* **809:**12-17.

Segawa Y, Tsuzuike N, Itokazu Y, Omata T, Inoue N, Nagasawa M, Nishioka H, Nakano Y, Kobayashi T and Kanda T (2001) Effects of a novel hepatoprotective drug, ZNC-2381, on fas-induced hepatocellular caspase-3 activity and apoptosis in mice. *Pharmacol* **62:**80-86.

Sugie N, Fujii N and Danno K (2002) Cyclosporin-A suppresses p53-dependent repair DNA synthesis and apoptosis following ultraviolet-B irradiation. *Photodermatol Photoimmunol Photomed* 18:163-8.

Tateyama H, Tada T, Hattori H, Murase T, Li WX and Eimoto T (1998) Effects of prefixation and fixation times on apoptosis detection by in situ end-labeling of fragmented DNA. *Arch Pathol Lab Med* **122:**252-255.

U.S. EPA (United States Environmental Protection Agency) (2002) Toxicological review of 1,1-dichloroethylene. U.S. EPA Region 8 and the Office of Solid Waste and Emergency Response, Washington, DC. EPA/635/R02/002.

Zimmermann KC, Bonzon C and Green DR (2001) The machinery of programmed cell death. *Pharmacol Ther* **92:**57-70.

Footnotes

a) This work was supported by Grant MOP 11706 from the Canadian Institutes of Health Research (P.G.F.).

b) **Address correspondence to:** Dr. Poh-Gek Forkert, Department of Anatomy and Cell Biology, Queen's University, Kingston, Ontario, Canada K7L 3N6. E-mail: forkertp@post.queensu.ca

Fig. 1. Hepatocytes isolated from murine liver 2 h after treatment with DCE (125 mg/kg) or DCE and CyA (50 mg/kg) and incubated with JC-1 probe for 30 min. Mean (red/green) fluorescence (± S.D., $n = 3$), expressed as percentage of control, indicates ratio of high/low mitochondrial membrane potential. For positive control, some animals were treated with Gal/ET for 4 h. *, significantly different from the control ($p < 0.001$); **, significantly different from DCE treatment ($p < 0.001$).

Fig. 2. Western-blot analysis of cytochrome *c*. Cytosolic proteins were obtained from livers of control (lane 1), DCE-treated (lane 2) and DCE + CyA-treated (lane 3) mice 4 h after exposure. Each lane represents a typical sample from an individual animal. Protein bands were subjected to densitometric analysis, and the relative amounts of cytochrome *c* were determined by reference to the controls. Bars represent mean relative density (± S.D., $n = 3$). *, significantly different from the control ($p < 0.001$).

Fig. 3. Time-course of serum ALT activity after DCE (125 mg/kg) or DCE and CyA (50 mg/kg) treatment. Control mice were treated with corn oil. Data are expressed as mean ± S.D. of measurements from three separate experiments. *, significantly different from the control ($p < 0.001$).

Fig. 4. Caspase-9 activity in murine liver. Data are expressed as mean ± S.D. of measurements from three separate experiments. To verify that the signal detected is due to caspase-9 protease activity, induced samples are incubated with caspase-9 inhibitor. *, significantly different from the control, and treatments with CyA + DCE and DCE with inhibitor ($p < 0.001$).

Fig. 5. Immunohistochemical detection of activated caspase-3 in murine liver. Staining was performed with a rabbit anti-active caspase-3 polyclonal antiserum.

Immunoreactivity in representative liver sections from mice treated with vehicle (A) or Gal/ET (B), or from mice treated with DCE for 12 h (C) or 24 h (D). Some mice were pretreated with CyA for 20 min before administration of DCE for 24 h (E). cv, central vein; pv, periportal vein. *Scale bar* = 200 μm.

Fig. 6. Histochemical analysis of DNA fragmentation using the TUNEL assay. (A) Control: Liver structure was histologically normal. TUNEL-positive cells were rare. (B) Gal/ET: Numerous positively-stained apoptotic hepatocytes scattered throughout the tissue. (C) DCE 12 h: TUNEL staining in some centrilobular hepatocytes. (D) DCE 24 h: TUNEL staining in centrilobular regions. Some TUNEL-positive hepatocytes were also observed in other areas of the parenchyma. (E) CyA + DCE 24 h: TUNEL staining was observed in centrilobular hepatocytes. Staining was confined to centrilobular regions. cv, central vein; pv, periportal vein. *Scale bar* = 200 μm.

Fig. 7. Representative H & E-stained liver sections from control (A) and DCE (125 mg/kg)-treated (B-D) mice. As positive controls for hepatocellular apoptosis, some mice were treated with 700 mg/kg galactosamine and 100 μg/kg endotoxin (Gal/ET) for 6 h (E). (A) Control: Liver architecture was histologically normal. Apoptotic and necrotic hepatocytes were absent. (B) DCE 12 h: Hepatocellular injury was not observed, compared with liver structure of controls. (C) DCE 24 h (×400): Mild centrilobular necrosis and eosinophilia were observed. Apoptotic hepatocytes were also identified in the centrilobular region. (D) DCE 24 h (×1000): Apoptotic hepatocytes (arrow) in centrilobular region demonstrating cell shrinkage, retraction of cell borders, and chromatin condensation and margination. Also, necrotic cells (arrowhead) exhibiting eosinophilia, swelling, vacuolation, and early stage karyorrhexis. (E) CyA + DCE 24 h:

Apoptotic (arrow) and necrotic (arrowheads) hepatocytes were observed in centrilobular regions. However, CyA pretreatment greatly reduced the number of hepatocytes undergoing apoptosis. (F) Gal/ET: Numerous apoptotic hepatocytes (arrows) showing typical morphological characteristics of apoptosis (i.e. cell shrinkage, chromatin condensation and/or margination, apoptotic bodies). cv, central vein; pv, periportal vein. *Scale bars* A-C, 200 µm; D-F, 20 µm.

JPET Fast Forward. Published on March 17, 2004 as DOI: 10.1124/jpet.104.066019
This article has not been copyedited and formatted. The final version may differ from this version.

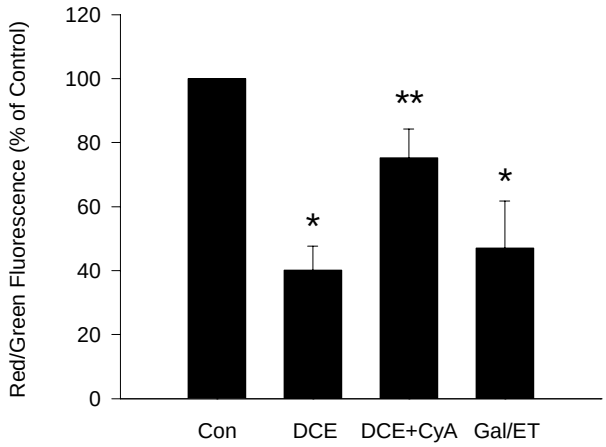

Figure 1
Martin and Forkert

JPET Fast Forward. Published on March 17, 2004 as DOI: 10.1124/jpet.104.066019
This article has not been copyedited and formatted. The final version may differ from this version.

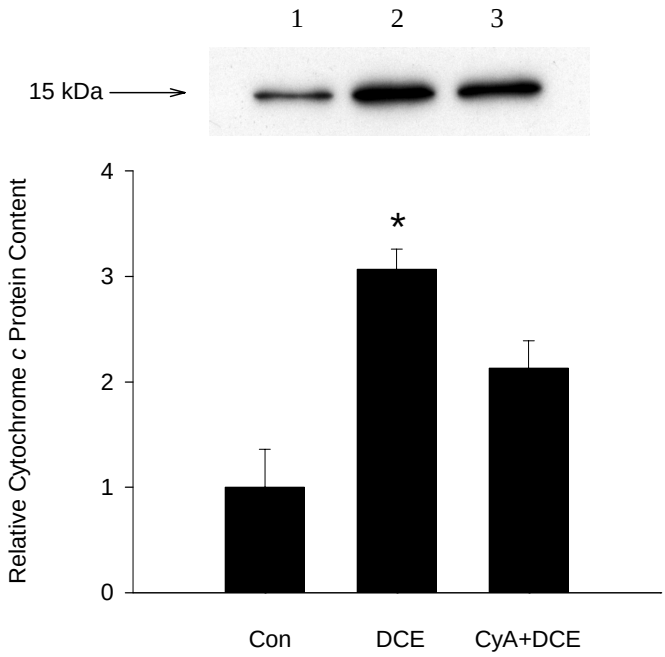

Figure 2

Martin and Forkert

JPET Fast Forward. Published on March 17, 2004 as DOI: 10.1124/jpet.104.066019
This article has not been copyedited and formatted. The final version may differ from this version.

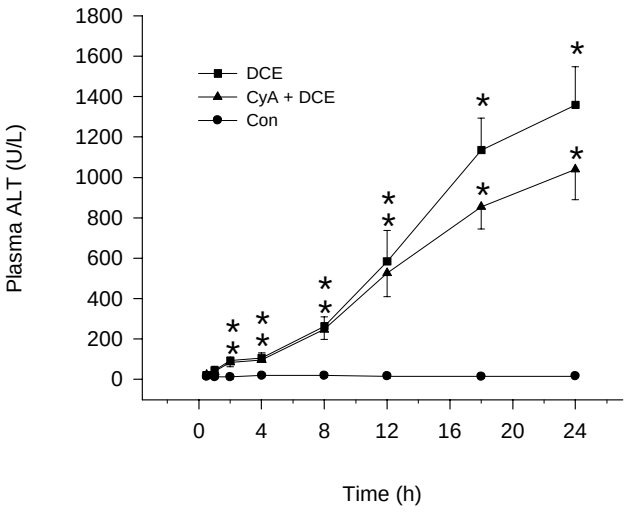

Figure 3
Martin and Forkert

JPET Fast Forward. Published on March 17, 2004 as DOI: 10.1124/jpet.104.066019
This article has not been copyedited and formatted. The final version may differ from this version.

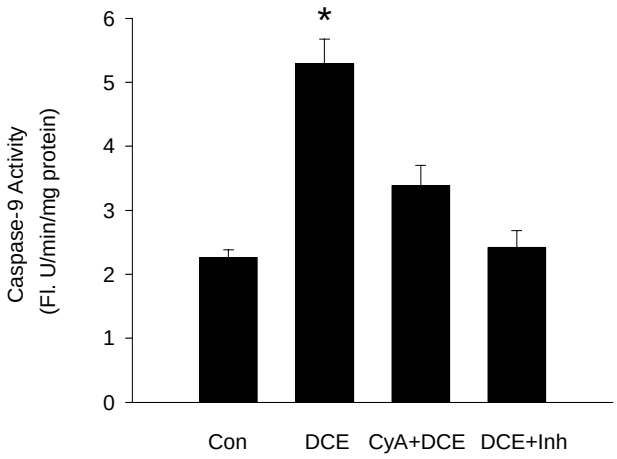

Figure 4
Martin and Forkert

JPET Fast Forward. Published on March 17, 2004 as DOI: 10.1124/jpet.104.066019
This article has not been copyedited and formatted. The final version may differ from this version.

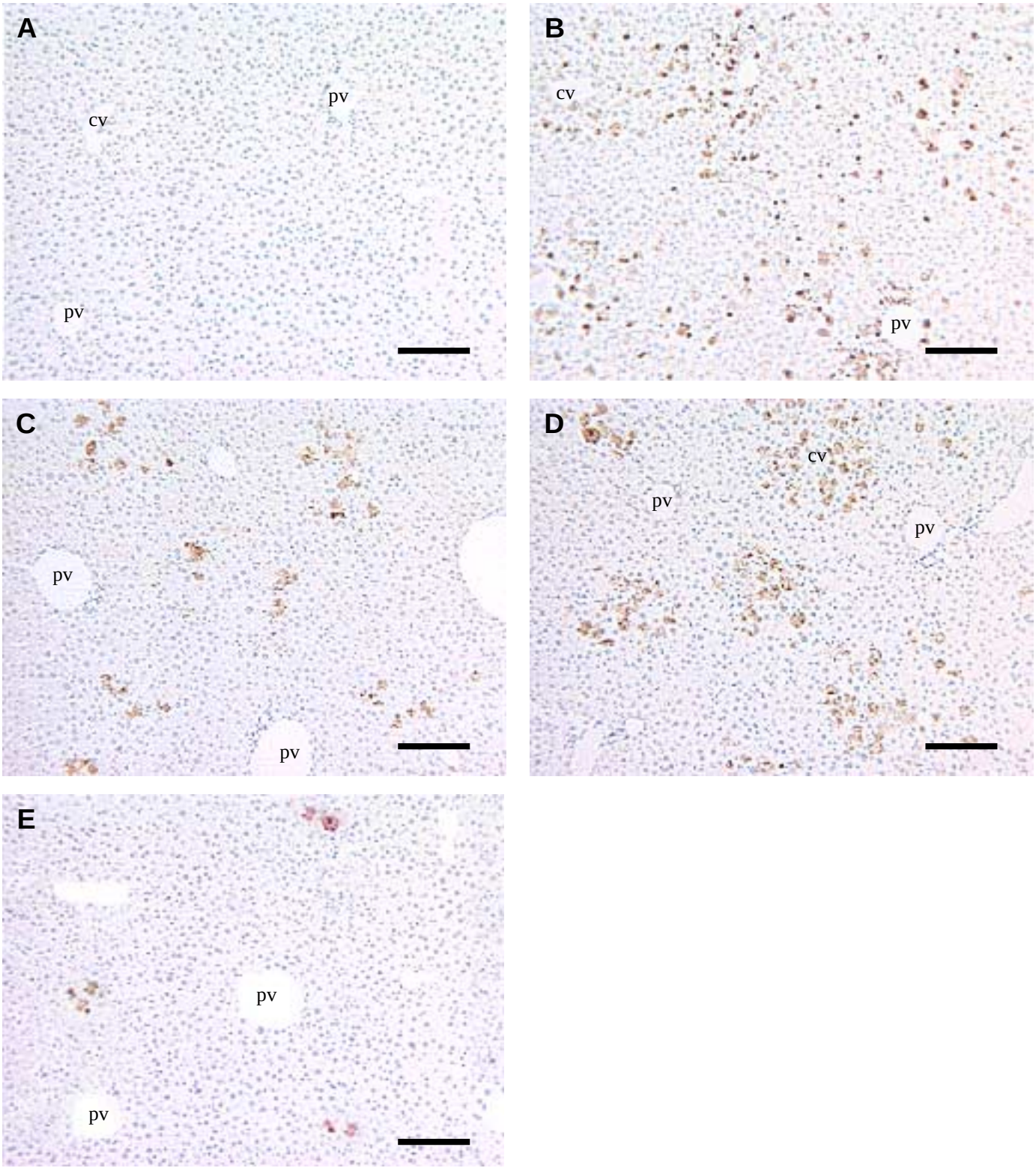

Figure 5
Martin and Forkert

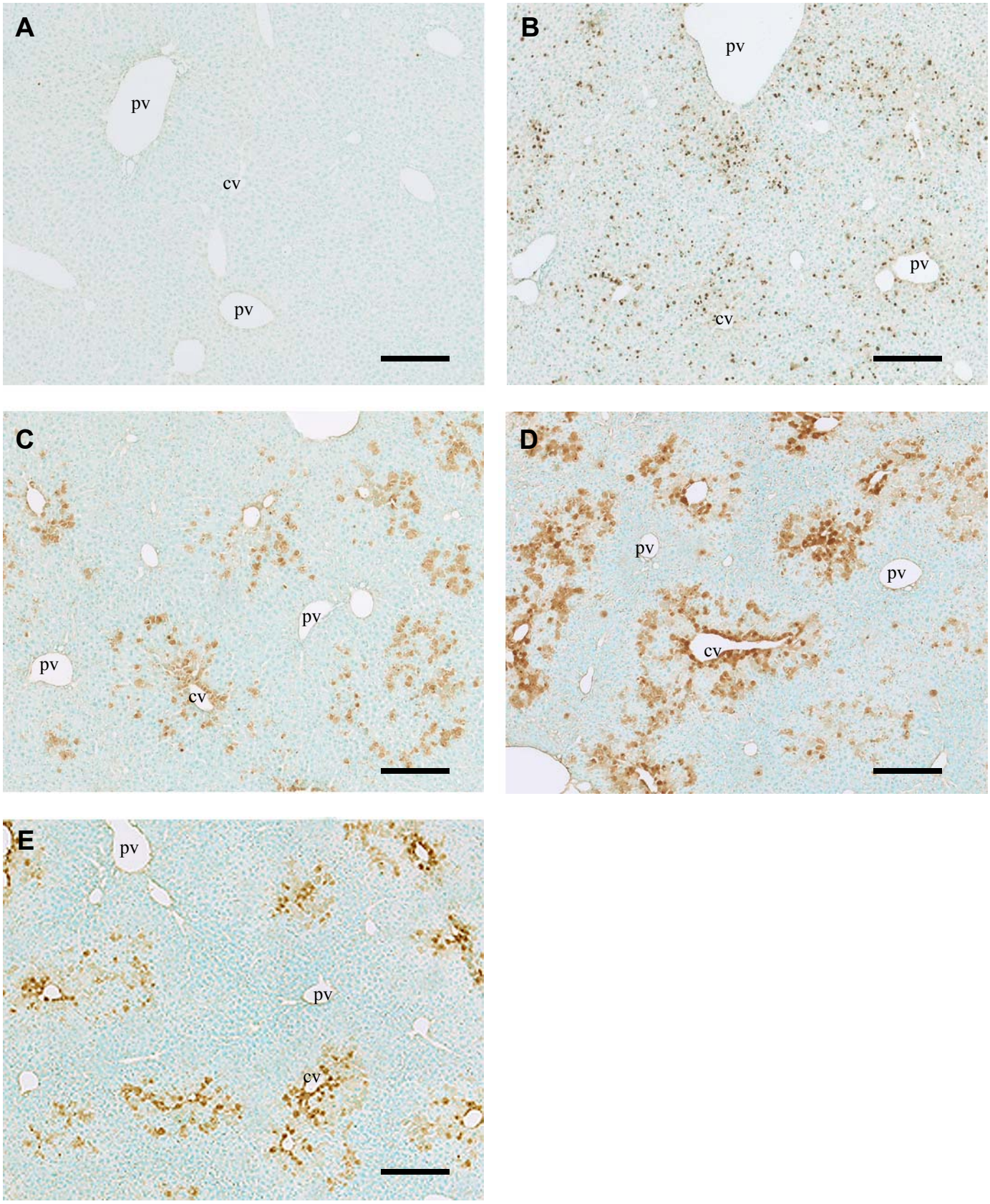

Figure 6
Martin and Forkert

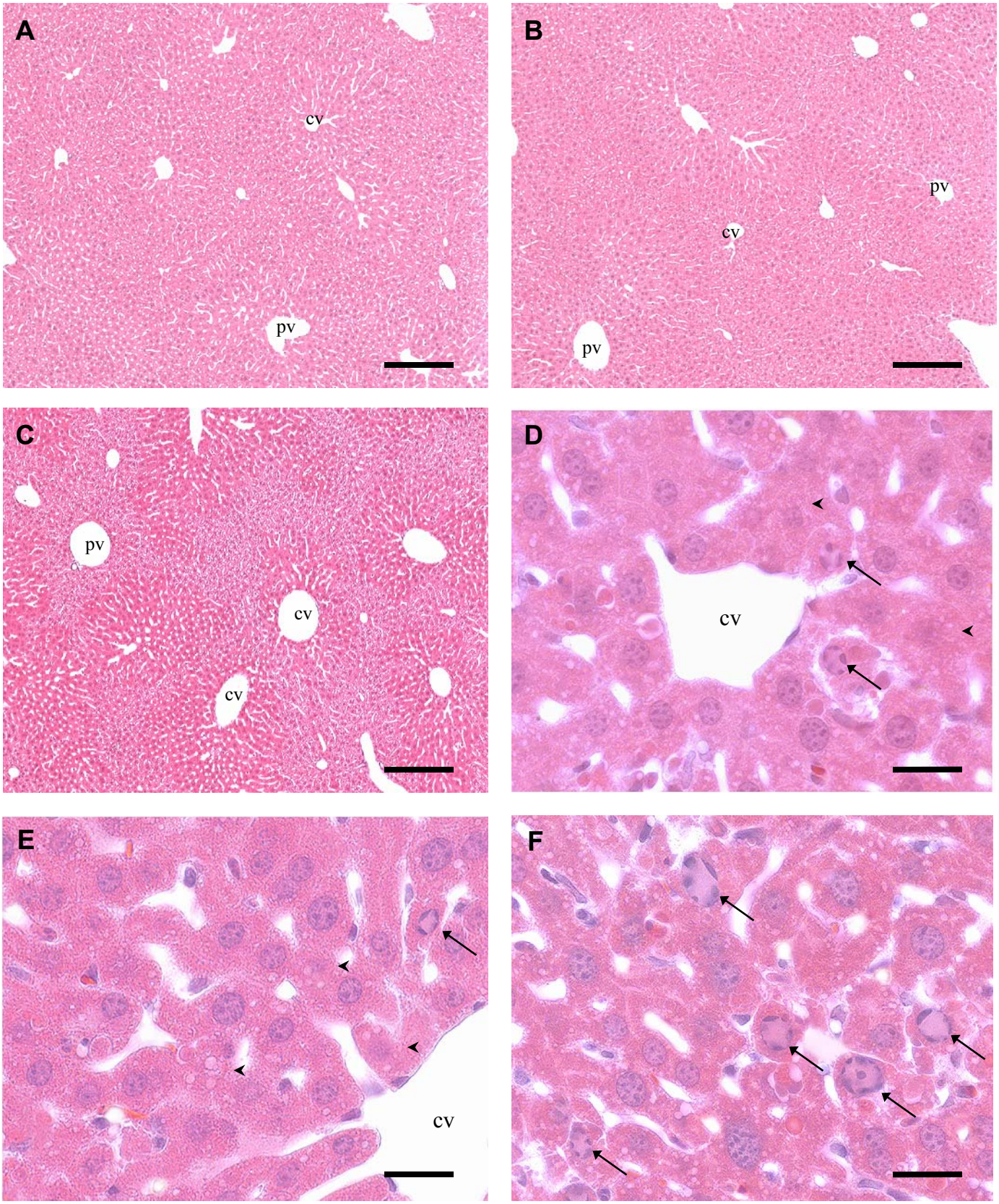

Figure 7
Martin and Forkert